Effects of delayed ettringite formation on reinforced concrete structures

Yvan Thiebaut, Stéphane Multon, Alain Sellier, Laurie Lacarriere, Laurent Boutillon, Djemal Belili, Lionel Linger, François Cussigh, Sofiane Hadji

HAL Id: hal-02155138
https://hal.insa-toulouse.fr/hal-02155138

Submitted on 13 Jun 2019

Effects of delayed ettringite formation on reinforced concrete structures

Yvan Thiebaut [a,b] , Stéphane Multon [a], Alain Sellier [a], Laurie Lacarrière [a], Laurent Boutillon [b], Djemal Belili [c], Lionel Linger [b], François Cussigh [d], Sofiane Hadji [e]

[a] *Université de Toulouse, LMDC (Laboratoire Matériaux et Durabilité des Constructions), UPS/INSA Génie Civil, 135 avenue de Rangueil, 31077 Toulouse Cedex 04, France*

[b] *Vinci Construction Grands Projets, Direction Scientifique, 5, cours Ferdinand-de-Lesseps 92 851 Rueil-Malmaison Cedex, France*

[c] *Cofiroute, 12-14 rue Louis Blériot. 92500 Rueil-Malmaison Cedex, France*

[d] *Vinci Construction France, 61 avenue Jules Quentin 92730 Nanterre, France*

[e] *Sixence Concrete, 24 rue Jean-Baptiste Huet 78350 Jouy-en-Josas, France*

Abstract

The prediction and reassessment of mechanical behaviour of reinforced structures affected by delayed ettringite formation (DEF) is a major challenge for structure managers. Firstly, several experimental tests were performed in laboratory to study the influence of both uni and tri-axial reinforcements on DEF expansion. Strain decreases in reinforced directions were observed, proving that DEF expansion under restraint is anisotropic. Cracks were observed parallel to the restrained directions. No strain transfert occurs from restrained directions to other ones. Secondly, data provided by these results are used to fit a numerical finite element model taking into account both chemical and mechanical aspects of DEF. Finally, an element of a DEF damaged structure is modelled with the whole model and compared to on site observations.

1   Introduction

Delayed ettringite formation (DEF) is a pathology that can occur in cementicious material under certain circumstances, resulting in expansion and damage [1]–[4]. In the context of reinforced structures, expansions decrease in restrained or loaded directions [2]–[6]. Reassessment and prediction of the mechanical behaviour of such structures are necessary. To do so, both non linear reinforced concrete behaviour and DEF impacts have to be modelled [7], [8]. The finite element model proposed by Sellier et al. takes into account creep and drying strains, localised and diffuse damages and internal pressures [9], [10]. Anisotropic behaviour of DEF expansions under anisotropic stresses is considered through independent plasticity criteria in each principal direction of stress. Before structural application, investigations were conducted to quantify the reinforcements and stresses influence on expansive concrete. Some authors studied effects of homogeneous restraint imposed by external reinforcements on immersed mortar prisms (40×40×160 mm) affected by DEF [3]. In other studies, reinforced concrete beams (610×914×5486 mm and 250×500×3000 mm) in heterogeneous hydric and mechanical conditions were considered [4], [6], [11]. In all these studies, expansions decreased in restrained directions. Complementary experimental study was necessary to extend those existing results to reinforced "pathologic" concrete. Non-reinforced, uni-axially and tri-axially reinforced prisms (100×100×500 mm) were exposed to a thermal cycle reaching 80°C and then stored in heated and non-renewed water, in homogenous thermal, mechanical and saturation conditions. Measurements of alkali concentration evolution in the storage bath due to leaching were made along the immersion period. Strains were regularly measured on the concrete surface with a calibrated extensometer. Materials, experimental set-up and conditions are presented in the first part of this article. Focus is then made on the model used in this study, especially on DEF mechanical modelling. The last section is dedicated to experimental results analysis, specimens modelling and reassessement of a reinforced concrete beam affected by DEF.

Proc. of the 12th fib International PhD Symposium in Civil Engineering
Aug 29 to 31, 2018, Czech Technical University in Prague, Prague, Czech Republic

1

2 Experimental investigation on reinforced concrete

2.1 Materials, curing conditions and storage

Experiments were performed on concrete with 410 kg/m3 of standard Ordinary Portland Cement CEM I 52.5 R (Table1 - left) and a water/cement ratio of 0.48. Non-reactive regarding Alkali-Silica Reaction (NF P 18-590) siliceous aggregates were used, supplied from Palvadeau quarry (France). Cement composition was obtained by Inductively Coupled Plasma - Optical Emission Spectrometry (ICP-OES) and chromatography analysis (Table 1 - right). Sodium hydroxide, NaOH, was added to the mixing water at a content of 5.0 kg/m3 of concrete.

Table 1　　Concrete composition (left) and cement chemical composition (right).

Component	Proportion (kg/m^3)	Oxides	Chromatography and ICP-OES analysis
Cement	410	SiO_2	20.1
Water	197	Al_2O_3	4.52
Sand 0/0.315	93.5	Fe_2O_3	2.37
Sand 0.315/1	174	CaO	64.6
Sand 1/2	184	MgO	0.78
Sand 2/4	196	SO_3	3.19
Gravel 4/8	188	K_2O	0.16
Gravel 8/12.5	878	Na_2O^*	0.15 *(before NaOH addition)*
NaOH addition	5.0	Na_2O_{eq}	0.25 *(before NaOH addition)*
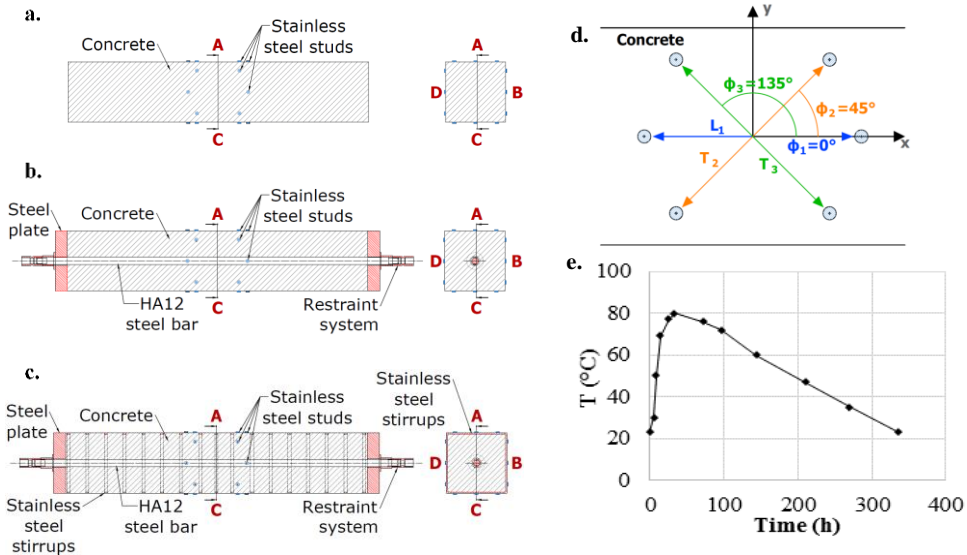
Fig. 1　　Non-reinforced (a.), axially reinforced (b.) and triaxially reinforced (c.) specimens (100×100×500 mm). Strain measurement orientation on concrete surface (d.).

A 14 days long thermal autogeneous treatment has been applied to the specimens after casting. The temperature increased from 23 to 80°C in 33 hours, decreased slowly from 80 to 72°C in 63 hours and returned from 72 to 23°C in 240 hours (Fig. 1 - e). The specimens were then stored at 23°C and 50% of relative humidity during 14 additionnal days. After that period, they were immersed in agitated, non-renewed water maintained at 38°C. The concrete/water volume ratio of the storage bath was constant

and equal to 0.23. Complementary physicochemical investigations, which are not detailed here in order to focus on mechanical aspects, have been made to provide data for numerical modelling.

2.2   Experimental set-up and measurements

Specimens were 100×100×500 mm prisms. Stress-free expansions were studied on plain prismatic specimens (Fig. 1 - a). In the case of DEF expansion under uni-axial restraint (Fig. 1 - b), a HA12 central longitudinal reinforcement was added in order to reach a section ratio between steel and concrete equal to 1.14%. Steel plates and restraint systems were added in order to improve longitudinal bars anchoring. Finally, tri-axially restrained specimens were composed of a HA12 central longitudinal reinforcement and external transversal stirrups distributed along the specimens (Fig. 1 - c). The transversal reinforcement ratio was equal to 0.68%. An extensometer was used for strain measurements. Stainless steel studs were glued on each face of the specimens. As the specimen width was not sufficient to allow direct measurements of transversal strains, some studs were glued forming angles of 45° and 135° with the longitudinal direction (Fig. 1 - d). Regular strain measurements were performed during the 333 days of specimen immersion.

2.3   Characterization

Tensile tests were performed on HA12 steel bars used as longitudinal reinforcements and their Young's modulus, yield strength and ultimate strength were 220 GPa, 505 MPa and 609 MPa, respectively. Table 2 presents the concrete Young's modulus, compressive and tensile strength. A minimum of three tests for each were performed on cylindrical specimens, submitted or not to heat treatment. A decrease of modulus and strength was observed, probably due on one hand to the impact of heat treatment on the microstructure development during hydration and on the other hand to differential thermal expansion between paste and aggregates, damaging the Intefacial Transition Zone.

Table 2   Heated (80°C) and non-heated (20°C) concrete characterization 28 days after casting.

Specimens designation	E (MPa)	Rc (MPa)	Rt (MPa)
20 °C-28d	40170 ± 550	40.0 ± 1.6	3.9 ± 0.4
80 °C-28d	35420 ± 270	31.3 ± 0.9	3.0 ± 0.3

3   DEF modelling principle

3.1   General mechanical modelling principle
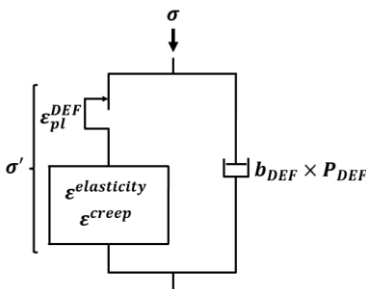
Fig. 2   Idealized rheologic scheme for DEF poromechanical model

When precipitating in the finite volume of porosity, delayed ettringite crystals act on pore edges. This internal pressure provoques matrix microcracking, leading to expansion. Compressive stresses in concrete (induced by loading or restraint due to reinforcement) can prevent microcracking apparition and propagation. The model used is dedicated to numerical simulation of non linear reinforced concrete behaviour taking into account strains due to creep and drying, localised and diffuse damages and internal pressures, including the one induced by DEF. A poromechanical framework is considered to manage interactions between phenomena: expansive products formed in pores acts on the solid matrix as

an internal pressure, which leads to creep and damage in tension, as schemed in Fig. 2. Reversible creep modelling relies on a Kelvin solid rheologic module when permanent creep is modelled thanks to a Maxwell visco-elastic fluid rheologic module. Water effects on concrete strains, such as drying creep, are modelled through a poromechanical capillary pressure theory: tension between liquid/gas water and solid matrix are assimilated to intraporal pressure. Numerous plasticity criteria are used to assess plastic strains. Localised cracking in tension and crack reclosure are managed by three Rankine criteria, one on each principal directions. Three sets of three others Rankine criteria are used to model diffuse matrix cracking due to alkali-silica reaction, DEF and water capillary pressure. Finally, failure in shear/compression is modelled through a Drucker Prager criteria with non associated flow. Damage comes along with each plastic phenomena described above, with creep and with temperature. The main aspects of DEF mechanical modelling are broached below.

3.2 DEF internal pressure

A poromechanical law is used to relate the intraporal pressure P_{DEF} with the difference between the volume of delayed ettringite ϕ_{DEF}, assessed from a chemical model, and the volume available for delayed ettringite precipitation (1). The volume available for delayed ettringite precipitation is composed of a fraction of the initial accessible porosity $\phi_{v,\,DEF}$, of the volume created by poral strains under pressure and external load $(tr(\varepsilon)\text{-}tr(\varepsilon_{pl}))$, and of the volume created by DEF diffuse microcracking $(tr(\varepsilon_{pl}^{DEF}))$. The Biot coefficient approximation b_{DEF} is obtained thanks to a homogenization method. The link between the difference of volumes and the intraporal pressure is made by the Biot's modulus M_{DEF}, assessed from the Biot coefficient and the compressibility moduli of the delayed ettringite and of the matrix deprived of the volume occupied by the delayed ettringite.

$$P_{DEF} = M_{DEF}\left(\phi_{DEF} - \phi_{V,\,DEF}\left(\frac{P_{DEF}}{\widetilde{R}_0^{DEF}}\right) - tr(\varepsilon_{pl}^{DEF}) - b_{DEF}\left(tr(\varepsilon) - tr(\varepsilon_{pl})\right) \right)^+ \quad (1)$$

$$\text{DEF internal pressure} = M_{DEF} \times \left[\text{Total delayed ettringite volume} - \text{Delayed ettringite in initial porosity} - \text{Delayed ettringite in microcracks} - \text{Delayed ettringite in porosity strains} \right]$$

3.3 DEF plasticity criteria and swelling anisotropy under restraint

If the intraporal pressure exceeds the solid skeleton strength in the case of an unloaded material, diffuse inelastic strains appear, corresponding to microcracking (ε_{pl}^{DEF} in Fig. 2 and eq. (1)). To numerically do so, three plastic Rankine criteria applied on principal stresses directions are used (2). The maximal stress value due to DEF intraporal pressure in the solid skeleton strength of the material is obtained mutiplying this pressure P_{DEF} by a stress concentration factor C, and is compared to the effective tensile strength $\widetilde{R}_I^t$. In the case of a loaded material, only negative total undamaged stresses $\left\langle \widetilde{\sigma}_{I \in [I,II,III]} \right\rangle^-$ (i.e. compression) are taken into account. In presence of anisotropic compressive loading, the plastic swelling associated to these cracks becomes anisotropic because the criteria have different values (Fig. 3).

$$f_I^g = C \times P_{DEF} - \widetilde{R}_I^{DEF} + \langle \widetilde{\sigma}_I \rangle^- \; avec \; I \in [I, II, III] \quad (2)$$
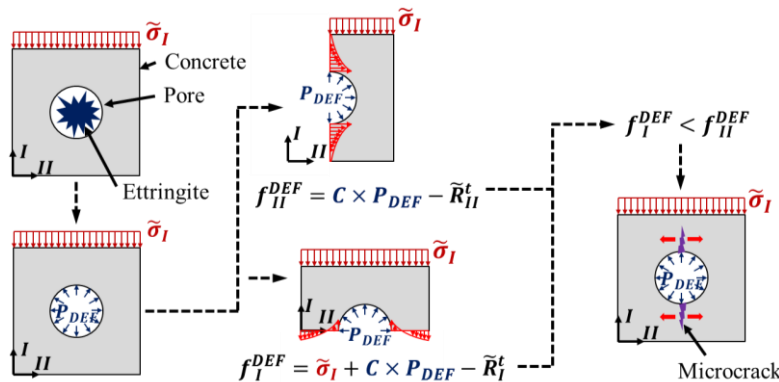
Fig. 3   Anisotropic cracking induced by an anisotropic compressive loading.

3.4 Distributed reinforcements

Model application to reinforced concrete structures could be complicated by the precision needed to mesh those reinforcements. A solution involves considering their structural effects as equivalent to the ones due to orthotropic distributed reinforcements. This method, avoiding explicit meshing of reinforcements, has been used in this article. Different reinforcements can be considered simultaneously with different orientations if necessary. Reinforcement plasticity and relaxation were modelled [12]. Perfect bond between matrix and reinforcements were considered in the cases of application presented below.

4 Analysis and modelling

4.1 Experimental and numerical results

For each case of reinforcement, experimental and numerical expansions were plotted on the same figure (Fig. 4). First, the focus is made on the analysis of the experimental results (cross symbol). Final longitudinal and transversal strains of 0.59% and 0.66%, respectively, were reached in the case of non-reinforced concrete (Fig. 4 - a), confirming observations made by Bouzabata et al. [3] concerning isotropic behaviour of DEF expansion in stress-free conditions. Effects of reinforcements on expansion are visible comparing the longitudinal strains of non-reinforced and uni-axially reinforced concrete (Fig. 4 - b). In this last case, reinforced direction exibits strains lower than 0.24% (decrease of about 60%). Cracks were observed parallel to the restrained directions. The longitudinal strain decrease is similar for the tri-axially reinforced concrete specimens (Fig. 4 - c). Stainless steel stirrups limited greatly transversal expansions, from 0.66% in stress-free conditions to 0.33% when restrained. Consequently, DEF expansion under anisotropic restraint is anisotropic. Moreover, uni-axially reinforced specimens exibit transversal strains slightly lower than ones of non-reinforced specimens. Longitudinal restraint has no major impact on transversal expansion: no strain transfer occurs. Comparison between longitudinal expansions of uni-axially, equal to 0.24%, and tri-axially reinforced specimens, equal to 0.21% seems to confirm that each direction could be considered independent from the restraint applied on the others. Nevertheless, some authors [3] observed on longitudinally restrained specimens that transversal expansions were slightly larger than for stress-free specimens, but without sufficient gap to consider a complete transfer of DEF expansions from loaded to free directions. Bouzabata et al.'s experimental program was made on highly reactive mortar samples (free expansions reached 2.3%): both the differences of material used in each study and their reactivity could explain these distinct phenomena.

Numerical results were obtained using several input data provided by the cement composition, concrete formulation and characterization, curing and storage conditions, and reinforcement characteristics. Alkali content in the intraporal water of the specimens was assessed with a diffusion model. The main parameters of alkali diffusion in concrete were fitted on experimental measurements of leached alkali in the storage water. Delayed ettringite volume evolution was provided by a chemical model using sulfate and aluminium initial contents, temperature, porosity saturation and alkali evolution as input data [13]. Then, the mechanical model described in chapter 3 has been used to simulate DEF effects on concrete specimens. In the case of structure requalification, expansion tests on non-reinforced concrete extracted from reinforced structures are mostly made years after casting and provide informations on residual expansion only. In this context, the most reliable data available for model calibration and validation are the strains and cracks distribution, opening and orientation, measured directly on the damaged structures. So, it appeared here more relevant to calibrate the model mainly on experimental expansions of reinforced specimens. Stress-free expansions are slightly underestimated (Fig. 4 - a): after 361 days of immersion, numerical strains are equal to 0.51% versus 0.59% and 0.66% for experimental longitudinal and transversal strains, respectively. Expansion kinetics is consistent regarding to experimental results. No clear numerical distinction occurs between longitudinal and transversal strains. Both longitudinal and transversal expansions of uni-axially reinforced specimens are well-assessed (Fig. 4 - b): in the reinforced direction, numerical and experimental strains are respectively 0.21% and 0.24% and are 0.57% and 0.58% in stress-free transversal direction. Concerning tri-axially reinforced specimens, a parametric study was made on stainless steel characteristics because no tensile test has been performed on it. Young's modulus value was supposed equal to 200 000 MPa. Two cases are presented here. On the one hand, yield strength and strain hardening coefficient were equal 160

MPa and 52 000 MPa, respectively. On the other hand, yield strength and strain hardening coefficient were equal 600 MPa and 2 000 MPa, respectively. Whatever the case considered, both longitudinal and transversal strains remain slightly overestimated (Fig 4 - c). When low yield strength and high strain hardening coefficient are used, longitudinal strains are well assessed, equal to 0.23% numerically and 0.21% experimentally, but the gap between modelling and measurements is important in transversal direction with values of 0.46% and 0.33%, respectively. This difference is reduced considering the case of high yield strength and low strain hardening coefficient: assessed transversal strains are equal to 0.38%. Longitudinal expansion provided by modelling, equal to 0.26%, remains consistent with experimental ones.
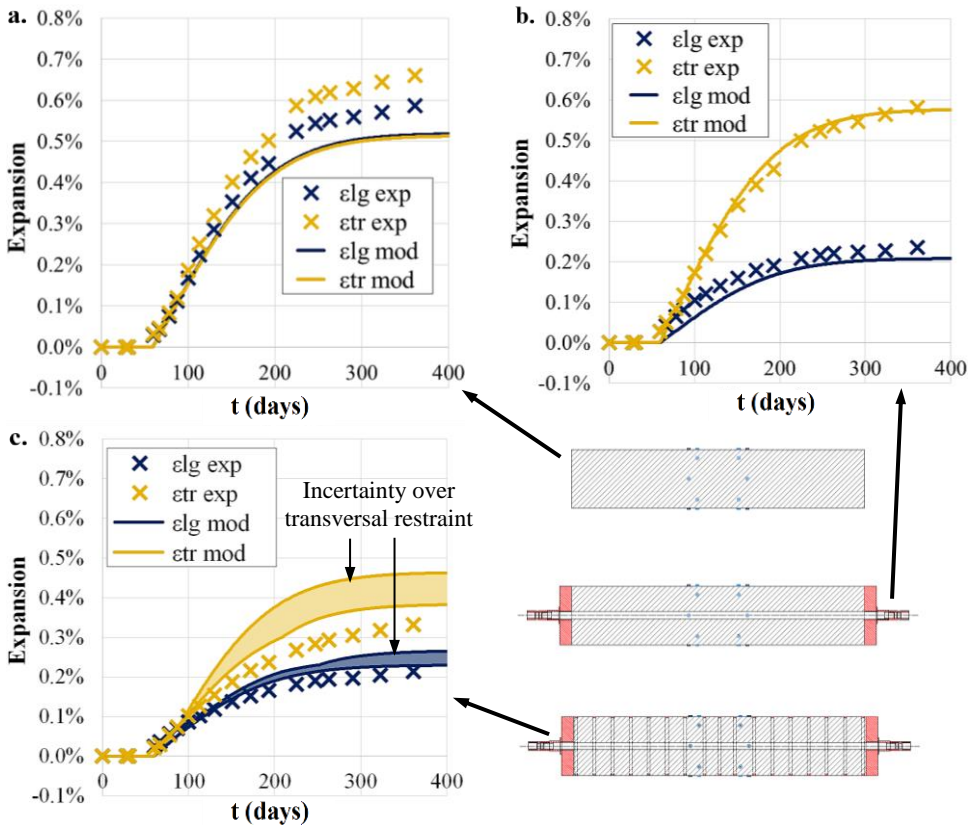
Fig. 4   Effect of restraint on expansion: experimental and numerical results

4.2   Application to reinforced concrete beam

The case of an isostatic reinforced concrete beam affected by DEF has been analysed. The beam length between posts is 9.2 m, with a transversal section of 1.0 m height and 0.7 m width (Fig. 5). Longitudinal reinforcement ratio is around 2%. In transversal direction, this ratio is equal to 0.35% in the first 1.6 m close to the post, and is only 0.17% in the central span. Their localisation was taken into account thanks to 0.1 m thick distributed orthotropic reinforcement zones on each edge of the beam. Two symetries has been used to decrease the calculation time. Homogeneous chemical expansion was considered, meaning that heat treatment, water content and alkali content were supposed homogeneous. Distributed vertical loading of 0.07 MN/m was applied on the upper surface of the beam. Posts have been modelled as punctual supports. Beam deformed shape before DEF beginning appears realistic (Fig. 6 - left). Curvature is positive (bent concave upward) because of the distributed loading applied on the upper part of the structure. Lower reinforcements are in tension, when upper ones are in compression (Fig. 7 - left). Localised macrocracks appeared in the lower part of the beam mid-span, because of tensile stress in concrete (Fig. 7 - right). Vertical displacement of the lower axis is close to 0.005 m.
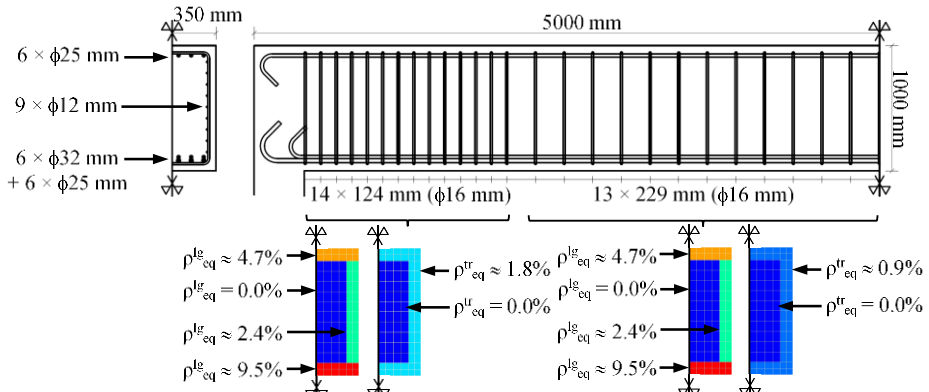
Fig. 5   Beam geometry and reinforcements. Equivalent distributed reinforcement ratio considered in the model.
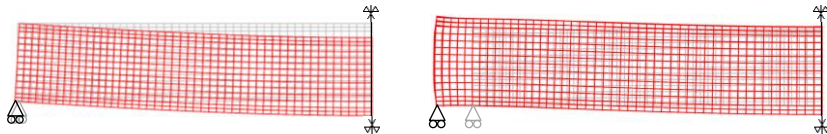
Fig. 6   Beam deformed shapes (amplification equal to 50) before (left) and after (right) DEF reaction.
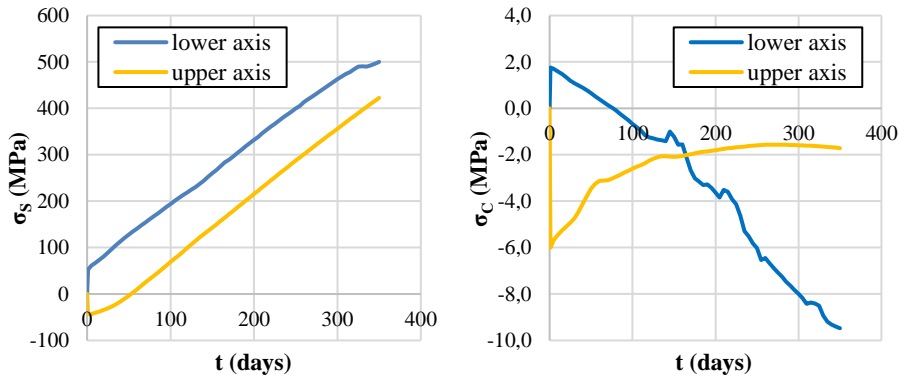
Fig. 7   Stress evolution in reinforcements (left) and concrete (right) in lower and upper axis of beam mid-span.

During DEF reaction, concrete expansion conducted to an increase of tensile stress in reinforcements resulting in compression in concrete. This phenomenon occurs mainly in heavily reinforced areas, such as the beam lower part (Fig. 7 - blue curves). After 140 days of expansion, compressive stresses lead to tensile macrocracks reclosure. Stress evolution in concrete lower part appears slightly unstable: it could be due to stress values projection from the Gauss points, where they are assessed, to the mesh, and to convergence issues induced by competition between DEF diffuse microcracks propagation and macrocracks reclosure. Because of asymmetric vertical distribution of longitudinal reinforcements in the beam, expansions are more important in upper than in lower area resulting in gradual beam curvature decrease (Fig. 6 - right). Initial vertical maximal displacement (caused by the mechanical loading) decreases from 0.005 m to less than 0.002 m in 350 days. Numerical results are consistent with on site observations: in some case, beam curvature can even change, from positive value before DEF beginning to negative value years later.

5   Conclusion

Interaction between reinforcements and expansions occuring in concrete affected by DEF has been studied in the present work. Experimental expansions of stress-free, uni-axially and tri-axially concrete specimens were studied and compared. Several important issues for the development of structural modelling have been highlighted. Firsly, expansion induced by DEF is isotropic in stress-free conditions. Secondly, experimental evidence of anisotropic concrete swelling due to DEF under anisotropic loading has been made. Cracks were mostly parallel to the restrained directions. And finally, no strain transfert occurs from restrained directions to others, meaning that each direction could be considered independent from the restraint applied on the others. The second part of this article has been dedicated to numerical modelling of these specimens. Concrete behaviour such as creep, plasticity and damage were considered along with DEF reactions and mechanical consequences. Numerical results appeared realistic compared to experimentation. Structural application has been made on a reinforced concrete beam affected by DEF. The consequences of interactions between reinforcements and expansions on structural mechanical behaviour appeared consistent with on site observations.

Acknowledgements

References

[1]   Z. Zhang, J. Olek, and S. Diamond, 'Studies on delayed ettringite formation in early-age, heat-cured mortars: I. Expansion measurements, changes in dynamic modulus of elasticity, and weight gains', *Cem. Concr. Res.*, vol. 32, no. 11, pp. 1729–1736, Nov. 2002.

[2]   X. Brunetaud, L. Divet, and D. Damidot, 'Impact of unrestrained Delayed Ettringite Formation-induced expansion on concrete mechanical properties', *Cem. Concr. Res.*, vol. 38, no. 11, pp. 1343–1348, Nov. 2008.

[3]   H. Bouzabata, S. Multon, A. Sellier, and H. Houari, 'Effects of restraint on expansion due to delayed ettringite formation', *Cem. Concr. Res.*, vol. 42, no. 7, pp. 1024–1031, Jul. 2012.

[4]   M. M. Karthik, J. B. Mander, and S. Hurlebaus, 'Deterioration data of a large-scale reinforced concrete specimen with severe ASR/DEF deterioration', *Constr. Build. Mater.*, vol. 124, no. Supplement C, pp. 20–30, Oct. 2016.

[5]   B. Burgher, A. Thibonnier, K. J. Folliard, T. Ley, and M. Thomas, 'Investigation of the internal stresses causes by delayed ettringite formation in concrete', Center for Transportation Research, the University of Texas at Austin, Technical report 0–5218, 2008.

[6]   D. J. Deschenes, O. Bayrak, and K. J. Folliard, 'ASR/DEF-damaged bent caps : shear tests and field implications', Ferguson Structural Engineering Laboratory - University of Texas at Austin, Austin, Texas, Technical report 12–8XXIA006, Aug. 2009.

[7]   N. Baghdadi, F. Toutlemonde, and J.-F. Seignol, 'Modélisation de l'effet des contraintes sur l'anisotropie de l'expansion dans les bétons atteints de réactions de gonflement interne', in *Conférence AUGC, Bordeaux*, 2007.

[8]   E. Grimal, A. Sellier, S. Multon, Y. Le Pape, and E. Bourdarot, 'Concrete modelling for expertise of structures affected by alkali aggregate reaction', *Cem. Concr. Res.*, vol. 40, no. 4, pp. 502–507, Apr. 2010.

[9]   A. Sellier, S. Multon, L. Buffo-Lacarrière, T. Vidal, X. Bourbon, and G. Camps, 'Concrete creep modelling for structural applications: non-linearity, multi-axiality, hydration, temperature and drying effects', *Cem. Concr. Res.*, vol. 79, pp. 301–315, Jan. 2016.

[10]   P. Morenon, S. Multon, A. Sellier, E. Grimal, F. Hamon, and E. Bourdarot, 'Impact of stresses and restraints on ASR expansion', *Constr. Build. Mater.*, vol. 140, pp. 58–74, Jun. 2017.

[11]   R.-P. Martin, 'Analyse sur structures modèles des effets mécaniques de la réaction sulfatique interne du béton', PhD thesis, Université Paris-Est, 2010.

[12]   P. Chhun, A. Sellier, L. Lacarriere, S. Chataigner, and L. Gaillet, 'Incremental modeling of relaxation of prestressing wires under variable loading and temperature', *Constr. Build. Mater.*, vol. 163, pp. 337–342, 2018.

[13]   A. Sellier and S. Multon, 'Chemical modelling of Delayed Ettringite Formation for assessment of affected concrete structures', *Cem. Concr. Res.*, vol. 108, pp. 72–86, Jun. 2018.